International Journal on Magnetic Particle Imaging
Vol 9, No 1, Suppl 1, Article ID 2303011, 5 Pages

Infinite Science Publishing

Proceedings Article

Deep Generative Adversarial Network for Direct Super-resolution Magnetic Particle Imaging Reconstruction

Hui Zhang[a,b,d,e] · Jing Zhao[a,b] · Yusong Shen[c] · Jie Tian[a,b,c,d,e,f,*]

[a]School of Engineering Medicine, Beihang University, Beijing,100191 China
[b]School of Biological Science and Medical Engineering, Beihang University, Beijing, 100191, China
[c]School of Computer Science and Engineering, Southeast University, Nanjing, 211189, China
[d]Key Laboratory of Biomechanics and Mechanobiology, Ministry of Education, Beihang University, Beijing, China
[e]Key Laboratory of Big Data-Based Precision Medicine, Ministry of Industry and Information Technology of the People's Republic of China, Beihang University, Beijing, China
[f]CAS Key Laboratory of Molecular Imaging, Institute of Automation, Chinese Academy of Sciences, Beijing, 100190, China
*Corresponding author, email: jie.tian@ia.ac.cn

Abstract

Due to the complex physical behavior of the nanoparticles, we propose to reconstruct the 2-D SPIO concentration image from the 1-D voltage signal in MPI scanning, and we aim to reconstruct the high-resolution 2-D image directly from the voltage signal by using the deep learning based generative adversarial network (GAN). We first built a large simulation image dataset, which includes 291,597 binary images and each image's corresponding MPI voltage signal simulated with our developed MPI simulation software MPIRF. By using the large simulation dataset, we trained a conditional-GAN model, which we termed "MPIGAN", that can successfully convert the 1-D MPI voltage signal to the high-resolution MPI image directly and precisely. Experiment results showed that, compared to the traditional methods, our proposed MPIGAN could better retrieve the fine-scale structure of the patterns of images from the 1-D voltage signals, and could achieve better reconstruction performance in both visual and quantitative assessments, e.g., SSIM, MSE, PSNR. Our study provides a promising end-to-end AI solution for efficient and high-resolution magnetic particle imaging reconstruction.

I. Introduction

Magnetic Particle Imaging (MPI) is an emerging imaging technique based on physical interactions between time-varying magnetic fields and superparamagnetic nanoparticles (MNPs) [1]. Two different methods are primarily used for magnetic particle image reconstruction. One relies on measurement of the system matrix [2]. However, the measurement of system matrix is really time consuming. Besides, the system matrix needs to be explicitly set up and stored in memory beforehand, which is memory-consuming and leads to relatively long reconstruction times. For these reasons, some model-based methods, such as the x-space method, were proposed to reduce the computational time as well as improve the reconstruction performance [3]. However, the model-based approaches are idealized and neglect the relaxation of the particles.

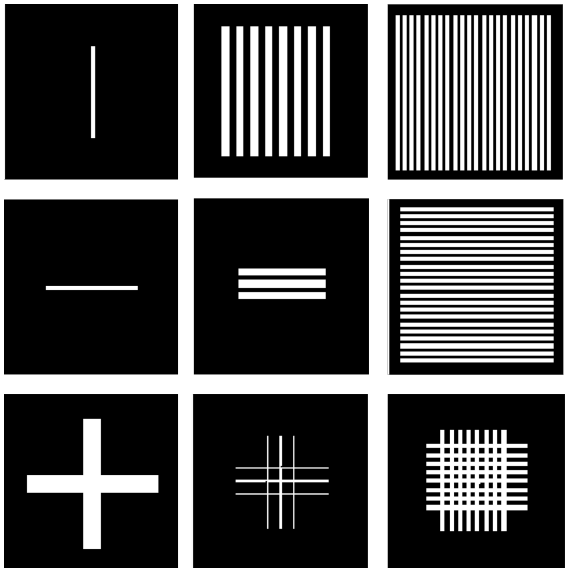

Figure 1: Selected images from the MPI simulation dataset.

The machine learning method of neural network has recently been introduced for MPI 2-D image reconstruction [4]-[11]. In MPI, convolutional neural networks have been used for reconstructing hybrid 1-D [4] and simulated 2-D data [5][6], and three frequency components [7]. A deep image prior has also been used to reconstruct measured 3D MPI data [8]. Recently, Generative adversarial networks (GANs) have been introduced in the machine learning community as an excellent image generative model. Compared to neural network, which aims for 'classification' task, GANs emphasizes image generation. Since it was proposed in 2014, GANs have proven to be very successful for generating high-quality images [12][13], not only for natural images, but also for medical images. Despite the success of GANs for image reconstruction such as super-resolution synthesis [14], and for improving the 3D imaging temporal resolution of projection MPI [15], there still lack a GAN model for high-resolution magnetic particle image reconstruction directly from the detected magnetic particle signals.

In our current study, we propose a novel GAN architecture, which we name MPIGAN, to reconstruct high quality 2-D images directly and quickly from collected magnetic particle signals.

II. Material and methods

In our study, we first built a large simulation image dataset and generated each image's corresponding one-dimensional MPI voltage signal. By using the dataset, we were able to train our generative model MPIGAN for MPI image reconstruction.

II.I. Large simulation dataset for MPI generation

In order to build our large simulation dataset, we first created a binary image dataset. The dataset contains a total of 291,597 images, including three forms of pattern design: bars arranged with parallel vertical (97,199 images), parallel horizontal (97,199 images), and both directions crossed (97,199 images). The bars in the images varied in number, width, spacing and length to simulate phantoms for MPI. As shown in Figure 1, the white area in the image indicates the location contains magnetic nanoparticles and the black area indicates the background. The size of the images is 128 × 128 pixels.

We then used our developed MPI simulation software MPIRF [16] to generate each binary image's corresponding one-dimensional MPI voltage signal from the receive coil. Assuming that the receive coil is homogenous everywhere and the magnetic particles are in thermal equilibrium, as in equation (1), the induced voltage of the receive coil can be formulated as

$$u(t) = -\mu_0 m_o \rho^R \beta \left[\left(H^D \right)'(t) \right] \int_{\text{object}} c(l) \mathscr{L}' \left[\beta \, H(l,t) \right] dl. \tag{1}$$

with

$$\beta = \frac{\mu_0 m}{k_B T^p}, \tag{2}$$

where μ_0 is the permeability of free space, m_o is the modulus of the magnetic moment of a single particle, ρ^R is the receiver coil sensitivity, β is a constant that represents the intrinsic property of the magnetic nanoparticle, k_B denotes the Boltzmann constant and T^p denotes the particle temperature. H^D is the driving field strength, G is the selected field gradient, c is the particle concentration, $\mathscr{L}'$ is the derivative of Langevin function, and H is the superposition field strength of the selection field and drive field at time t and point l. After obtaining the one-dimensional signal, it is normalized and then used as the input signal for MPIGAN.

The simulation of the voltage signal was based on the Langevin model of paramagnetism. The field of view (FOV) was defined to have a size of 12.8 mm×12.8 mm, the particle size was 30 nm, the particle saturation magnetization was 0.6 T, the particle concentration was 50 mmol/l, and the temperature of particle was 293.15 K. A selection field gradient of 2.0 T/m was generated along the x-direction, and an excitation field gradient of 12 mT with 24.51 KHz frequency was applied in the same direction. A selection field gradient of 2.0 T/m was generated along the y-direction, and an excitation field gradient of 12 mT with 26.042 KHz frequency was applied in the same direction. The repetition time was 652.8 μs and the sample frequency was 2.5 MHz. We used 2D-excitation for simulating the data. We only used the signal in the x direction as the input to MPIGAN, and the dimension of the input signal is 1×1632. The signal received by the

10.18416/ijmpi.2023.2303011

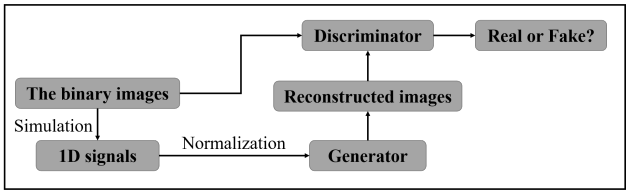

Figure 2: Schematic illustration of the reconstruction method.

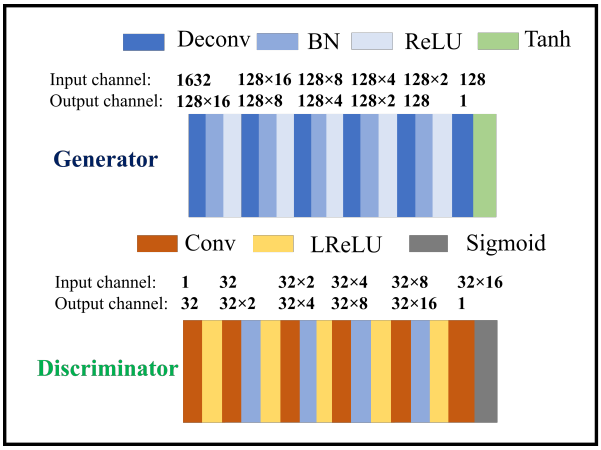

Figure 3: Schematic illustration of the MPIGAN architecture.

receive coil is entirely from the voltage signal generated by the particles, and will not receive the signal from the excitation field.

By creating the large binary image dataset and simulating each image's corresponding MPI voltage signal from receive coil, we were able to train a deep-learning-based generative model that can realize the high-resolution MPI image reconstruction from the original one-dimensional MPI voltage signal, as shown in Figure 2.

II.II. MPIGAN

Our MPI reconstruction framework is based on the conditional GAN [12], which can realize the reconstruction of two-dimensional images from the one-dimensional vector. By using the large binary image dataset and their corresponding simulated voltage signals, we trained a GAN model, which we termed 'MPIGAN', to convert the induced 1D MPI voltage signal to the 2D MPI image. A schematic illustration of the detailed MPIGAN architecture is depicted in Figure 3.

Our MPIGAN architecture was loosely inspired by [12] to complete the reconstruction of one-dimensional data to two-dimensional images. DCGANs are an extension of GANs [13], in that convolutional layers are added to the generator and discriminator architecture to improve the stability of GAN-generated images.

The loss function of traditional GANs is equivalent to the Jensen-Shannon divergence. However, there is a serious problem with the Jensen-Shannon divergence. When the distributions between original data and the generated data do not overlap, the Jensen-Shannon divergence reaches zero and causes the model iteration stops. To improve the stability of training, we use Hinge loss in generator and discriminator to ensure that only those samples that are not reasonably distinguished from each other will have an effect on the gradient. The generator loss function also contains a constraint term, which is the mean absolute error (MAE) between the generator output and the ground truth image weighted with a control parameter λ_G, summed with the binary cross entropy of the discriminator's decision using the generator output. Here, λ_G is set to the value of 10.

For obtaining a reliable MPIGAN, the large MPI dataset associated with its simulated voltage signals was randomly divided into two splits at a rough ratio of 30:1, 282,525 pairs were used for training (n = 291,597, 96.9%) and 9072 pairs for testing (n = 291,597, 3.1%). In both training and testing sets, the proportion of images containing horizontal bar, vertical bars, and two directions crossed were the same and had a ratio of 1/3. The generator model was trained with the stochastic gradient descent (SGD) optimization algorithm. The generator learning rate was set to 2×10^{-4}, the discriminator learning rate was set to 2×10^{-3}, and the batch size was set to 400. The network was iterated for a fixed number of 300 epochs until the loss function reached a stable state. For the generator G of GAN model, each block except the last block consisted of one deconvolutional layer with 4×4 kernels followed by a batch normalization (BN), and subsequently by a rectified linear unit (ReLU) activation. ReLU activation was used for all layers of generator except for the output layer, which used Tanh activation. The discriminator D undertook a classification task to differentiate the reconstructed images from the ground truth. Each of which included a convolutional layer with 4×4 kernels followed by a batch normalization and a leaky ReLU layers, except for the first and last block. For the first block of D, no BN was used, convolution operation was followed by a leaky ReLU layer. For the last block of D, a convolutional layer was cascaded and the sigmoid activation function output the classification results. The input and output channels of deconvolutional and convolutional layer are shown in Figure 3.

III. Experiments and Results

To verify the performance of our proposed framework for reconstructing MPI images, we compared the reconstruction of MPIGAN with system matrix (SM) and x-space method. SM establishes the relationship between the spatial tracer position and the frequency response. X-space method setup a direct mapping of the measure-

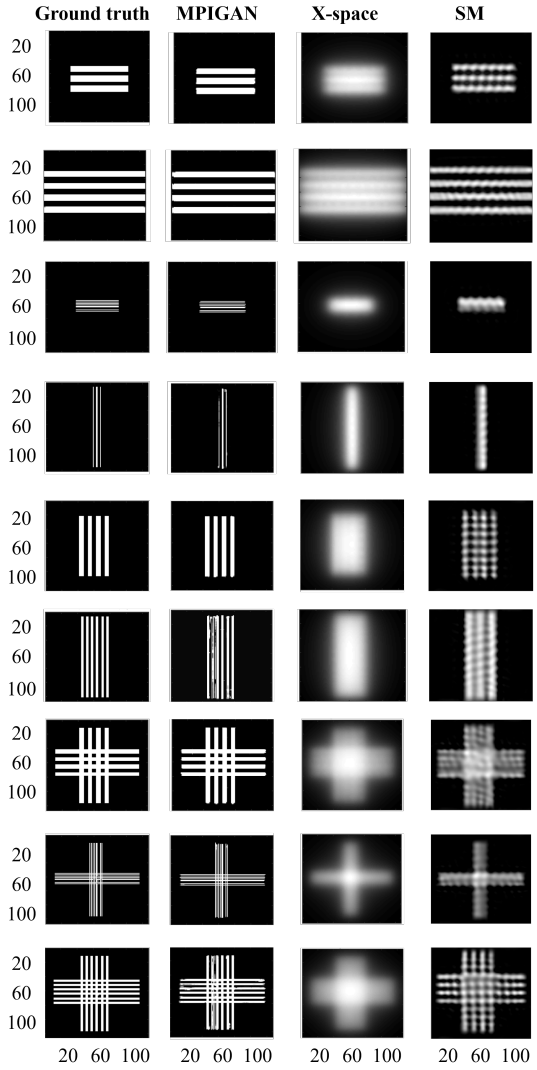

Figure 4: Random test set reconstructions using both conventional methods, as well as the proposed MPIGAN method. Left to right: ground truth, MPIGAN, x-space, and system matrix reconstruction.

ment signal to the corresponding spatial position. The choice of field-free point trajectories was Lissajous trajectory both in SM and x-space method, and the trajectory density parameter was set to 16. Specifically, in SM reconstruction, the Kaczmarz algorithm was used [16]. There was not frequency selection applied to the rows of the MPI system matrices. As for the x-space reconstruction method, we used the fully automated gridding to reconstruct the Lissajous trajectory, which refers to the article published by Ozaslan et al.[17].

Samples of reconstructed images using SM, x-space, and MPIGAN are visualized in Figure 4. As shown in the figure, images reconstructed with x-space are very blurry, and the patterns in the images cannot be distinguished from the background. The fine-scale information contained in the images is lost. The images reconstructed with SM look better, and were able to distinguish the bars with relatively close distance, but the reconstructed images contained stripped noise. In contrast, MPIGAN generates images that are visually close to the real image and retains the rectangular shape and spacing to the maximum extent, resulting in higher spatial resolution of the generated images compared to SM and x-space.

Table 1: Quantitative results of the comparison study using different methods.

	MPIGAN	SM	X-space
MSE	0.1307*	0.1432	0.1620
PSNR	10.2285*	8.9832	8.6078
SSIM	0.8070*	0.7843	0.5938

*indicates p<0.05

We also used three metrics to quantify the reconstruction performance of SM, x-space, and our proposed MPIGAN, which included peak signal-to-noise ratio (PSNR), structural similarity index measure (SSIM) [18] and mean square error (MSE). The results are shown in Table 1.

The metric values in the table were statistically tested by using permutation test. For each reconstructed image in the dataset, we randomly picked 1000 images other than the ground truth (distractor), and calculated the metric values between the distractor images and the reconstructed images. The procedure was repeated for each image in 10 images randomly selected from test set, and a distribution of metric values was created. We used the distribution to determine the probability (α) of obtaining the averaged metric values for the true image reconstruction against the null hypothesis that the metric value for reconstructing the ground truth is the same as distractor images ($p<0.05$).

IV. Discussion

In this study, we propose a large simulated dataset containing pairs of 2D MPI images and their corresponding simulated 1D MPI voltage acquisition signals. By using this dataset, we developed a deep-learning-based GAN model, which we termed 'MPIGAN', to realize direct high-resolution MPI reconstruction from voltage signals. MPIGAN outperformed system matrix and x-space in terms of the quality of the reconstructed image. Compared to previous studies using deep learning models to train a more precise super-resolution system matrix, our work provides an end-to-end solution for efficient and high-resolution MPI reconstruction. Though our ultimate goal is to train a robust end-to-end generative model for direct real measured data reconstruction. There are several limitations in our current study. One is that our simulated dataset for training the MPIGAN is binary images with only bar shapes, while in actual MPI scan, the par-

ticle concentration is presented as grayscale with irregular shapes. Another is that the distribution of the real measured MPI data was not fully considered in our GAN model, which greatly limits its application in measured data reconstruction. Finally, in our current study, MPI-based noise-model were not included in our GAN model training. In our next study, we will use gray-scale images containing more varied shapes to train our model. We will add various noise models to our dataset for model training to improve the robustness of our model. We will further develop more robust GAN model compatible to MPI image sequences with varied parameter settings.

V. Conclusion

To achieve fast reconstruction of MPI signals, we propose an MPIGAN model. Compared with other reconstruction methods, MPIGAN generates images with higher quality. Meanwhile, the model has been tested on simulated data only, and subsequently, we will further consider to prove the effectiveness of the model for data measured on real MPI scanners.

Acknowledgments

This work was supported by National Natural Science Foundation of China under Grant 81871511 and 62027901.

Author's statement

Conflict of interest: Authors state no conflict of interest. Informed consent: Informed consent has been obtained from all individuals included in this study. Ethical approval: The research related to human use complies with all the relevant national regulations, institutional policies and was performed in accordance with the tenets of the Helsinki Declaration, and has been approved by the authors' institutional review board or equivalent committee.

References

[1] A. Neumann, K. Gräfe, A. von Gladiss, M. Ahlborg, A. Behrends, X. Chen, J. Schumacher, Y.B. Soares, T. Friedrich, H. Wei, et al., Recent developments in magnetic particle imaging, J. Magn. Magn. Mater. 550 (2022) 169037.

[2] Gleich, B., Weizenecker, J. Tomographic imaging using the nonlinear response of magnetic particles. Nature 435, 1214–1217 (2005). https://doi.org/10.1038/nature03808

[3] Goodwill PW, Conolly SM. The x-space formulation of the magnetic particle imaging process: one-dimensional signal, resolution, bandwidth, SNR, SAR, and magnetostimulation. IEEE Trans Med Imaging. 2010;29:1851–1859.

[4] Chae B G. Neural network image reconstruction for magnetic particle imaging. ETRI Journal, 2017, 39(6): 841-850.

[5] Koch, P., Maass, M., Bruhns, M., Droigk, C., Parbs, T. J., & Mertins, A. (2019, March). Neural network for reconstruction of MPI images. In International Workshop on Magnetic Particle Imaging (pp. 39-40).

[6] von Gladiss, A., Memmesheimer, R., Theisen, N., Bakenecker, A.C., Buzug, T.M., Paulus, D. (2022). Reconstruction of 1D Images with a Neural Network for Magnetic Particle Imaging. In: Maier-Hein, K., Deserno, T.M., Handels, H., Maier, A., Palm, C., Tolxdorff, T. (eds) Bildverarbeitung für die Medizin 2022. Informatik aktuell. Springer Vieweg, Wiesbaden. https://doi.org/10.1007/978-3-658-36932-3_52

[7] Hatsuda, T., Takagi, T., Matsuhisa, A., Arayama, M., Tsuchiya, H., Takahashi, S., & Ishihara, Y. (2016). Basic study of image reconstruction method using neural networks with additional learning for magnetic particle imaging. International Journal on Magnetic Particle Imaging, 2(2).

[8] Dittmer, S., Kluth, T., Baguer, D.O., Maass, P. (2020). A Deep Prior Approach to Magnetic Particle Imaging. In: Deeba, F., Johnson, P., Würfl, T., Ye, J.C. (eds) Machine Learning for Medical Image Reconstruction. MLMIR 2020. Lecture Notes in Computer Science(), vol 12450. Springer, Cham. https://doi.org/10.1007/978-3-030-61598-7_11

[9] von Gladiss, A., Kramer, I., Theisen, N., Memmesheimer, R., Bakenecker, A. C., Buzug, T. M., & Paulus, D. (2022). Data augmentation for training a neural network for image reconstruction in MPI. International Journal on Magnetic Particle Imaging, 8(1 Suppl 1). https://doi.org/10.18416/ijmpi.2016.1611002

[10] Knopp, T., & Grosser, M. (2022, December). Warmstart approach for accelerating deep image prior reconstruction in dynamic tomography. In International Conference on Medical Imaging with Deep Learning (pp. 713-725). PMLR.

[11] Askin, B., Güngör, A., Alptekin Soydan, D., Saritas, E. U., Top, C. B., & Cukur, T. (2022). PP-MPI: A Deep Plug-and-Play Prior for Magnetic Particle Imaging Reconstruction. In International Workshop on Machine Learning for Medical Image Reconstruction (pp. 105-114). Springer, Cham.

[12] Mirza M, Osindero S. Conditional generative adversarial nets. arXiv preprint arXiv:1411.1784, 2014.

[13] Radford A, Metz L, Chintala S. Unsupervised representation learning with deep convolutional generative adversarial networks. arXiv preprint arXiv:1511.06434, 2015.

[14] Y. Gu, Z. Zeng, H. Chen, et al., MedSRGAN: medical imagessuper-resolution using generative adversarial networks, Multimed.Tool. Appl. 79 (2020) 21815–21840, https://doi.org/10.1007/s11042-020-08980-w.

[15] Wu, X., He, B., Gao, P., Zhang, P., Shang, Y., Zhang, L., ... & Tian, J. (2022). PGNet: Projection generative network for sparse-view reconstruction of projection-based magnetic particle imaging. Medical Physics.

[16] Shen Y, Hu C, Zhang P, et al. A novel software framework for magnetic particle imaging reconstruction. International Journal of Imaging Systems and Technology, 2022.

[17] Ozaslan AA, Alacaoglu A, Demirel OB, Çukur T, Saritas EU. Fully automated gridding reconstruction for non-Cartesian x-space magnetic particle imaging. Phys Med Biol. 2019 Aug 21;64(16):165018. doi: 10.1088/1361-6560/ab3525

[18] Wang Z, Bovik A C, Sheikh H R, et al. Image quality assessment: from error visibility to structural similarity. IEEE transactions on image processing, 2004, 13(4): 600-612.

